ELSEVIER

Journal of Power Sources 92 (2001) 56–64

JOURNAL OF POWER SOURCES

www.elsevier.com/locate/jpowsour

# Study of the influence of glycerol on the cathodic process of lead electrodeposition and on its morphology

I.A. Carlos*, M.A. Malaquias, M.M. Oizumi, T.T. Matsuo

*Departamento de Química, Universidade Federal de São Carlos, C.P. 676, 13565-905 São Carlos (SP), Brazil*

Received 2 May 2000; accepted 16 May 2000

**Abstract**

Potentiodynamic lead electrodeposition on 1010 steel was studied, so as to examine the influence of glycerol on the cathodic process of lead plating and, if possible to obtain films consistently with characteristics suitable for use in lead battery technology and corrosion protection. Under potentiodynamic conditions the lead deposits obtained on 1010 steel were not satisfactory for corrosion protection but could be transformed into high purity lead powder. Given the undercutting of the lead film during the anodic dissolution scan, it is suggested that an anodic pulse could be applied to peel off the lead film on 1010 steel. The 1010 steel substrate showed itself to be potentially useful as a cathode in the treatment of $Pb/H_2SO_4$ battery industry waste and in the production of lead powder, due to its low cost and non-adherence of lead films. With the help of scanning electron microscopy (SEM) photographs, an explanation has been offered for the influence of glycerol on the lead electrodeposition process. It was concluded that glycerol reduces the dendritic growth but does not favor the adherence of the electrodeposits. © 2001 Elsevier Science B.V. All rights reserved.

*Keywords:* Lead deposit; Glycerol; 1010 steel; Alkaline bath; Recovery

## 1. Introduction

Fragile lead films have important applications in various technological areas, for instance the production of high purity active material in acid battery plates [1] and various alloys [2]. Another application of lead films is in corrosion protection on steel alloys in industrial atmospheres and in containers used to transport corrosive material [3,4]. In this case, strong adherence of the deposit to the substrate is very important. Also, new methods have been developed for lead scrap recycling, in which new electrolytic solutions to carry out lead electrodeposition have been proposed and tested [5,6].

Electroplating of lead [7] has been accomplished from various acid solutions: nitrate, fluoroborate, fluorosilicate, perchlorate, pyrophosphate, acetate, etc. As most acid electrolytes are toxic, alkaline electrolytes are more appropriate from the environmental standpoint and great attention has been given to their application.

Weiping et al. [8,9] investigated the electrochemical process of lead electrodeposition from alkaline tartrate solutions and demonstrated that under proper conditions higher electrodeposition efficiency can be achieved. Also, they verified that the technological process is stable, without environmental pollution.

Calusaru [2] produced lead powder from an alkaline solution in the presence of glycerol and showed that this additive favors anode dissolution.

Morachevskii et al. [10] demonstrated that it is possible to use alkaline glycerol solutions to separate the active substance from battery plate grids, since glycerol increases the solubility of the sulfate–oxide fraction of the lead battery scrap.

It was shown in these studies [2,10] that glycerol hinders the passivation of the anode and dissolves the oxide fraction of the scrap. It would be invaluable to find out what influence glycerol has on the cathodic process of lead deposition, since this could affect the chemical, physical and morphological characteristics of the lead film.

Alkaline electrolytes are valuable not only from the point of view of environmental protection but also for their low corrosiveness compared to acid electrolytes. It should be remembered that electrodeposits can be contaminated by metal dissolved from the cathode [11,12], which can be detrimental in many applications, such as in high purity lead powder to be used in batteries. Furthermore, when lead electrodeposits are used to protect steel alloys against

* Corresponding author. Tel.: +55-16-260-8208; fax: +55-16-261-2081.
*E-mail address*: ivani@dq.ufscar.br (I.A. Carlos).


PII: S0378-7753(00)00525-5

corrosion, adherence of lead to substrate is essential. Then, dissolution of substrate in the initial moments of cathodic polarization would have a detrimental effect on the adherence of lead film. Therefore, alkaline electrolytes could be used for lead electrodeposition, for example, on steel alloy substrate, since at alkaline pH passivation occurs by oxide formation [13–15].

In this context we will examine the electrodeposition of lead on 1010 steel substrates, from an alkaline lead bath, in the presence and absence of glycerol, and whether the morphological characteristics of the lead films are acceptable and consistent to be used in the fields of batteries and corrosion protection.

## 2. Experimental

All chemicals were of analytical grade. Double distilled water was used throughout. Each electrochemical experiment was performed in a bath containing $Pb(NO_3)_2$+NaOH at various concentrations, in the presence and absence of 0.2 M glycerol. A 1010 steel disk (0.5 $cm^2$), a Pt plate and a Hg/HgO/2 M NaOH electrode with an appropriate Lugging capillary were employed as working, auxiliary and reference electrodes, respectively. The 1010 steel disk, from CSN Co., contained 0.044% P, 0.08% C, 0.3% Mn and 0.05% S. Immediately prior to the electrochemical measurements the 1010 steel alloy working electrodes were ground with emery paper, then rinsed with double distilled water. Potentiodynamic curves were recorded using a PAR model 366 potentiostat/galvanostat and a plotting system recorder. Electrochemical efficiency ($\phi_e$) was calculated from the ratio between dissolution and deposition charges. All experiments were carried out at room temperature (25°C). Scanning electron microscopy (SEM) micrographs were taken with a Carl Zeiss, Model DMS 940A and a Philips, Model X L 30 FEG electron microscopes.

## 3. Results and discussion

### 3.1. Electrodeposition of Pb on 1010 steel in absence of glycerol

Voltammograms for the stationary 1010 steel substrate in the plating bath at various lead concentrations and 2.0 M NaOH are shown in Fig. 1. In Fig. 1a there is a wave followed by a cathodic peak. This indicates that, for these values of deposition current density, it is possible to consider the chemical stage as coupled to mass transport, which limits the concentration of the species being deposited. Thus, it may be inferred that the reduction process occurs through $Pb^{2+}$ ions. Fig. 1b shows lead electrodeposition from 0.001 M $Pb^{2+}$+1.0 M $Na_2SO_4$. It can be seen that the voltammetric profile obtained corroborates Fig. 1a, supporting the proposed deposition mechanism through $Pb^{2+}$ ions.

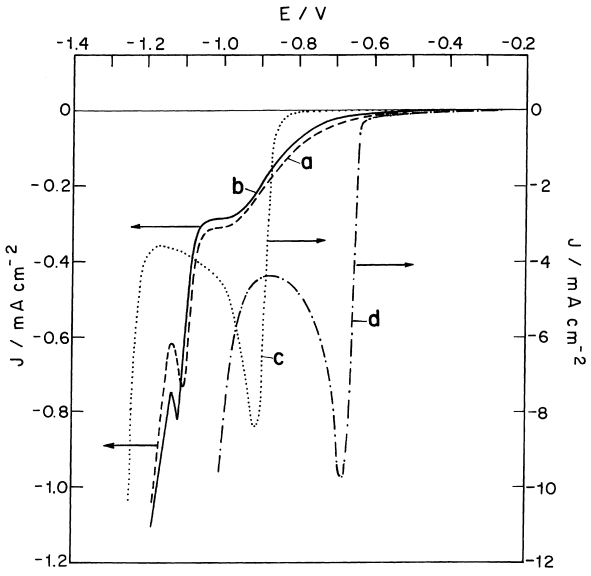


Fig. 1. Voltammetric curves for 1010 steel substrate in: (a) 0.001 M $PbNO_3$+2.0 M NaOH, (b) 0.001 M $PbNO_3$+0.10 M $Na_2SO_4$, (c) 0.050 M+2.0 M NaOH and (d) 0.100 M $PbNO_3$+2.0 M NaOH at 10 mV/s.

Fig. 1c and d show only the cathodic peak, characterized by a steep increase in current density, after which the current density decreases, due to mass transport limitation. Still in Fig. 1c and d, the increase in the current density to a further cathodic peak can be associated with hydrogen evolution and/or an increase in the area of deposit suggesting a second nucleation process. As the deposition process is characterized by higher exchange current density, this reduces the overpotentials of reaction, charge transfer and crystallization to low values. Hence, as the reaction overpotential is very low despite the lead ions being complexed, this implies that the reduction of lead ion occurs entirely through the complex species $[Pb(OH)_4]^{2-}$ and not the $Pb^{2+}$ ions.

It can be concluded from the results that for industrial purposes the deposition bath containing 0.1 M of $Pb^{2+}$+2.0 M NaOH is best, since it gives the highest rate of deposition.

It was observed that during the dissolution of the lead film (Fig. 2), undercutting of the deposit occurred at the top of the

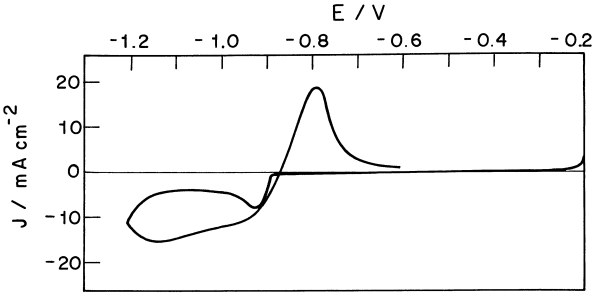


Fig. 2. Voltammetric curves for 1010 steel substrate in 0.100 M $PbNO_3$+2.0 M NaOH at 10 mV/s.

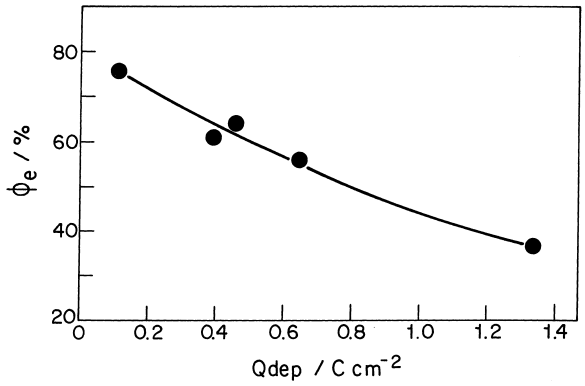


Fig. 3. Electrochemical efficiency ($\phi_e$) of lead electrodeposits obtained at different deposition charges from 0.100 M $PbNO_3$+2.0 M NaOH.

anodic peak. This behavior during the anodic dissolution process shows that the lead deposits are non-adhering.

As can be seen in Fig. 3, the electrochemical efficiency ($\phi_e$) of lead electrodeposits obtained at various deposition charges, from 0.1 M $Pb^{2+}$+2.0 M NaOH, decreases with increasing deposition charge, owing to undercutting of the lead deposit. These results also show that the undercutting becomes more intense at higher charge densities because the deposit is bulkier, denser and less adherent. The low adherence of the lead dendrite deposits on 1010 steel substrate is potentially useful since they can be detached from the electrode before their growth can cause short-circuiting. The resulting powdery deposit is highly pure lead suitable for use as active material in batteries. The undercutting of the lead film suggests that an anodic pulse could be used to favor peeling of the deposit from the 1010 steel.

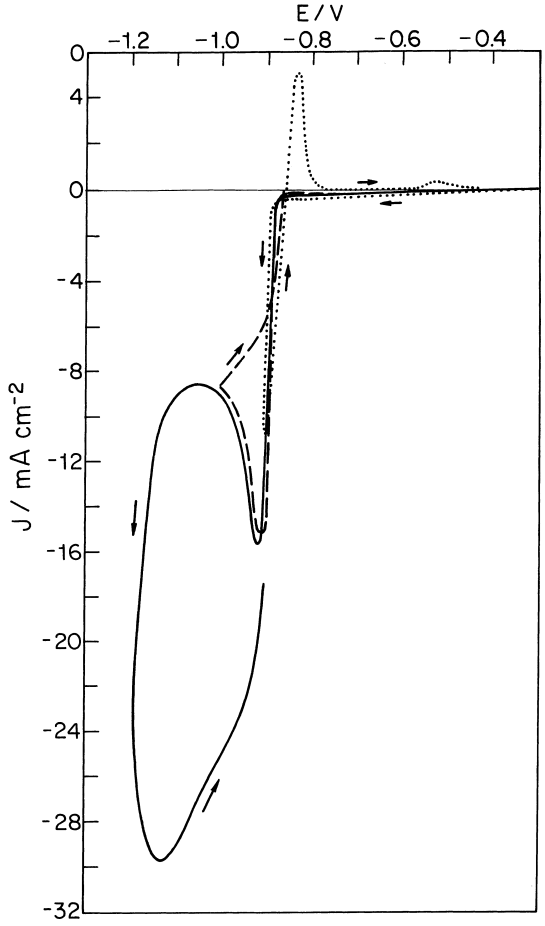


Fig. 5. Voltammetric curves for 1010 steel substrates in 0.100 M $PbNO_3$+2.0 M NaOH and effect of the cathodic potential limit values: −0.90 V (dotted line), −1.0 V (broken line) and −1.18 V (solid line) at 10 mV/s.

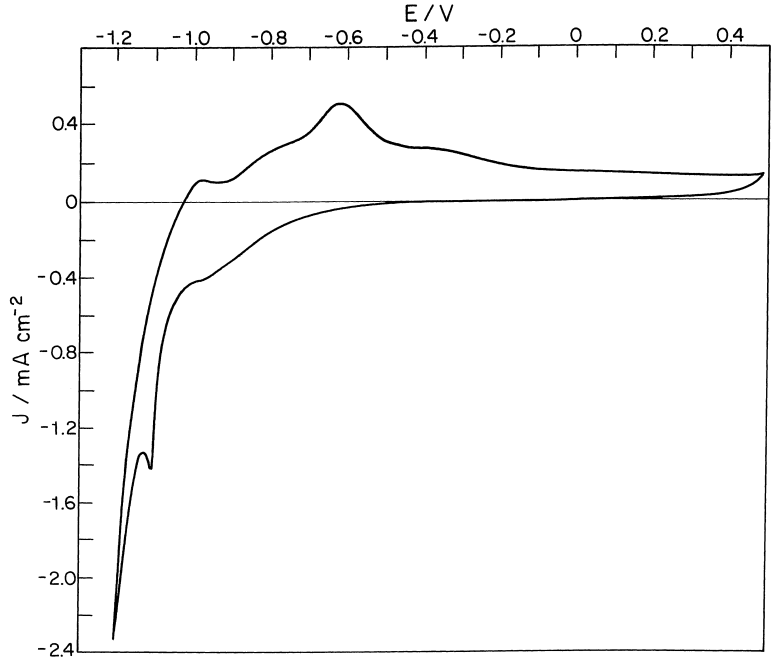


Fig. 4. Voltammetric curves for 1010 steel in 2.0 M NaOH at 10 mV/s.

The $H_2$ evolution overpotential, in the absence of the plating salts, was also studied on the 1010 steel electrode. The cathodic voltammogram produced with this substrate in 2.0 M NaOH, displayed in Fig. 4, shows no current up to approximately −0.5 V, suggesting that $H_2$ evolution is not a significant side reaction during the initial stages of the plating process. It is only important beyond the region of the cathodic peak (Fig. 1). Also, it can be verified on the anodic voltammogram that the 1010 steel is passivated, corroborating the findings of others [13–15]. This behavior is significant since it indicates that contamination of the lead electrodeposits with iron or other steel components does not occur in the initial moments of the cathodic scan of the lead deposition process.

To characterize the cathodic process better, the sweep was reversed at several potentials (Fig. 5). When the sweep was reversed at −0.90 V (Fig. 5, dotted line), the slight increase in cathodic current density, on the reverse, indicates a feeble nucleation phenomenon. After the lead deposition, the cathodic current decreases fast before the formation of an anodic peak followed by a hump. This hump corresponds to passivation of the lead film remaining on the steel electrode after the undercutting of the deposit. The characteristic features of nucleation, the crossover on the cathodic branch [16], can be observed better in Fig. 5 (broken line). Finally, at −1.18 V (Fig. 5, solid line), on the reverse scan, the current density increases indicating a large increase in the deposit area and a second nucleation. Also, the increase in the current density on the forward scan (Fig. 5, solid line) can be attributed to hydrogen evolution, as can be seen in Fig. 4, and not only to the increase in the deposit area.

To clarify the mechanism of the deposition process, a set of voltammograms were obtained from this bath at various sweep rates and they are presented in Fig. 6. The current density at the cathodic peak exhibits a steep increase with the sweep rate. This is because the higher the scanning rate, the lower the fall in concentration of $Pb^{2+}$ species at the metal/solution interface, and this leads to higher current densities. It can be inferred from these voltammogram features that the rate of lead deposition is controlled by mass transport in the regions beyond the cathodic peak.

Normally, the limiting current density ($I_L$), given by the equation [17]: $I_L=NFDC/\delta$, is around 20 mA/cm$^2$ for $C$=0.1 M, $D=10^{-5}$ cm$^2$/s and $\delta=10^{-2}$ cm. In the present

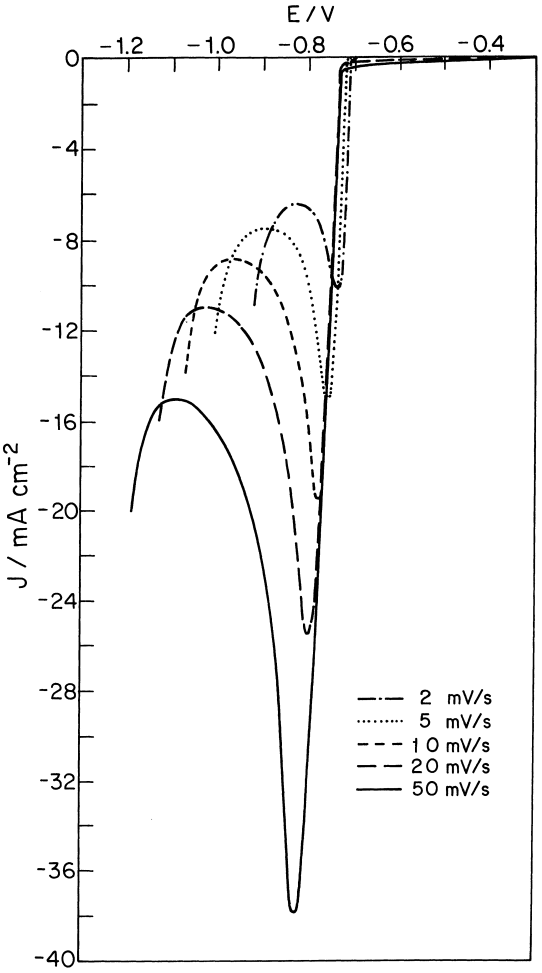


Fig. 6. Voltammetric curves for 1010 steel substrates in 0.100 M $PbNO_3$+2.0 M NaOH at various sweep rates.

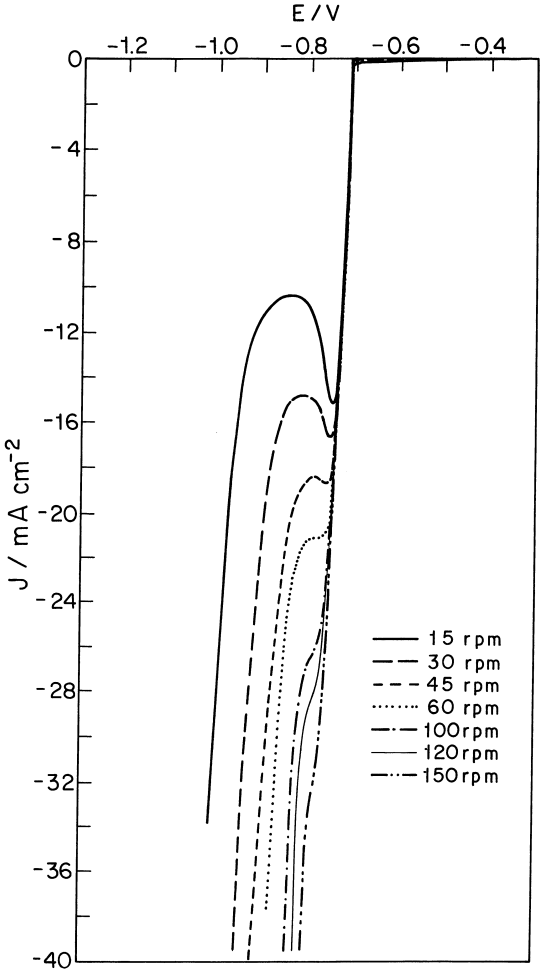


Fig. 7. Voltammetric curves for 1010 steel substrates in 0.100 M $PbNO_3$+2.0 M NaOH at various rotation speeds and at 5 mV/s.

case the limit current density is 10 mA/cm$^2$ with the stationary electrode, of the same order as this theoretical value. Thus, the idea of diffusion control is plausible.

To confirm the results obtained with the stationary electrode concerning the mass transport control of the deposition process, studies with a rotating disk electrode (RDE) were made. Fig. 7 displays the voltammetric curves with the RDE at various speeds of rotation. These results show that at the start of the deposition process there is no contribution from mass transport control, because the deposition current densities are independent of the speed of rotation. Only beyond the cathodic peak does mass transport become important. Comparing Figs. 6 and 7 (dotted line), the current densities on the RDE are much higher, indicating that the limiting current densities observed on the stationary electrode are due to mass transport limitation.

### 3.2. Electrodeposition of Pb on 1010 steel in the presence of glycerol

Fig. 8 shows voltammograms for the stationary 1010 steel substrate in the 0.1 M $Pb^{2+}$ plating bath at various NaOH concentrations and in the solutions: 0.6 M NaOH (Fig. 8a) and 2.0 M NaOH (Fig. 8b), all in the presence of 0.2 M glycerol.

Comparing Figs. 6 and 8 ($v$=10 mV/s), it can be seen that the presence of glycerol shifts the lead deposition potential to more cathodic values. Also, glycerol reduces significantly the deposition current density in the region of cathodic peak (Fig. 8, solid line). The reduction of the deposition current density can be interpreted as an inhibition of the deposition process in the region of cathodic peak, or a modification in the morphology of the deposit. The latter effect has been observed during copper electrodeposition from an alkaline glycerol plating bath, where inhibition of crystallite growth took place [15].

These results are very significant since the presence of glycerol in the deposition bath may lead to a better quality deposit.

It can be verified in Fig. 8, that the lead plating rate is not affected kinetically by hydroxide ion, since the current density magnitudes are the same at all $OH^-$ concentrations. Nevertheless, hydroxide ion does affect the plating rate thermodynamically, since the initial deposition potential changes to more cathodic values with increasing NaOH concentration. This probably occurs because of higher adsorption of glycerinate anions, since more of the glycerol is neutralized with the increase in NaOH concentration.

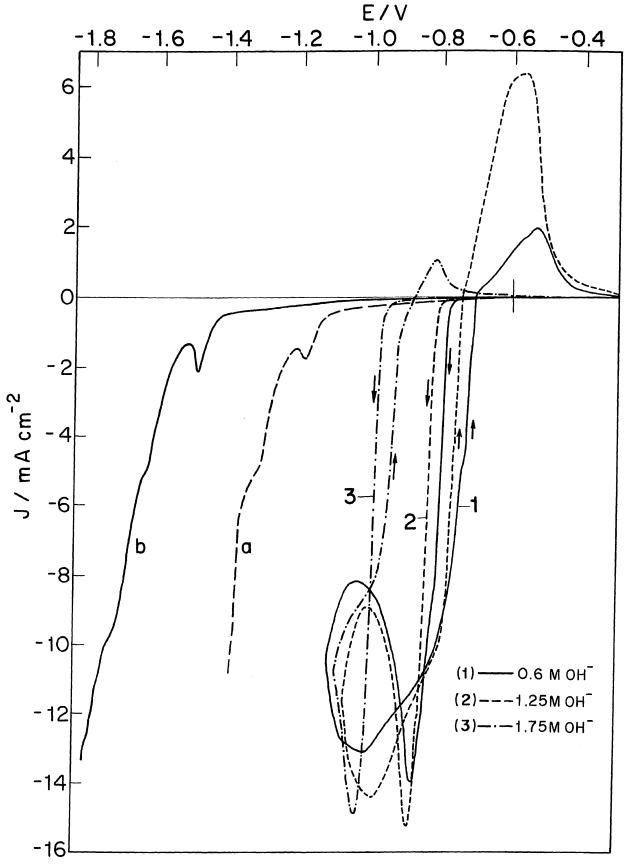


Fig. 8. Voltammetric curves for 1010 steel substrate in 0.100 M $PbNO_3$+0.2 M glycerol at various NaOH concentrations; curve 'a' (broken line): 0.600 M NaOH+0.2 M glycerol and curve 'b' (solid line): 1.75 M NaOH+0.2 M glycerol at 10 mV/s.

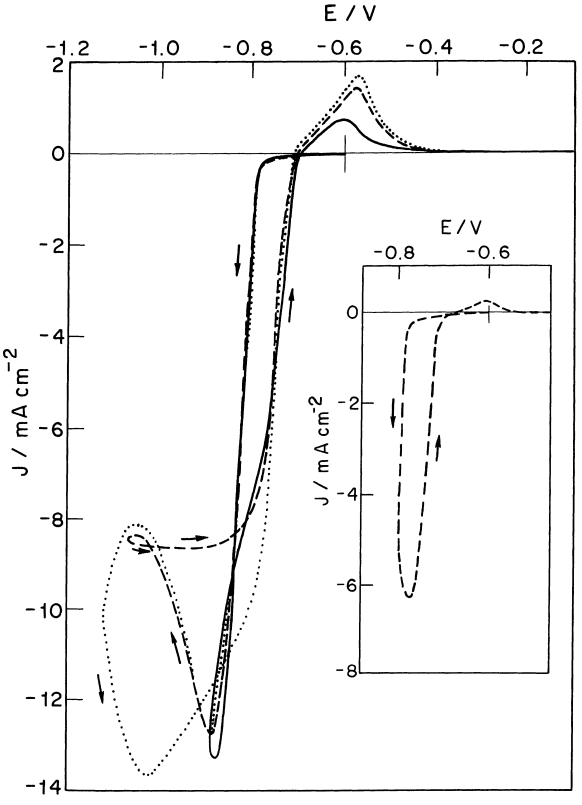


Fig. 9. Voltammetric curves for 1010 steel substrates in 0.100 M $PbNO_3$+2.0 M NaOH+0.2 M glycerol and effect of the cathodic potential limit values: −0.87 V (solid line), −1.07 V (broken line), −1.13 V (dotted line) and −0.80 V (insert) at 10 mV/s.

The $H_2$ evolution overpotential in the absence of the plating salts was studied, by taking voltammetric readings with the 1010 steel electrode in a bath containing 0.6 M NaOH (Fig. 8a) and 2.0 M NaOH (Fig. 8b) both in the presence of 0.2 M glycerol. As already observed in Fig. 4, $H_2$ evolution does not affect the voltammetric deposition of Pb in the initial moments of the process. It is only really significant at potentials beyond −1.3 and −1.7 V, for 0.6 and 2.0 M NaOH, respectively. Also, it can be seen that in 2.0 M NaOH the hydrogen evolution is more polarized than in 0.6 M NaOH, probably due to the higher concentration of glycerinate anions that may be adsorbed on the 1010 steel substrate.

It can be inferred from the results above that the presence of glycerol in the plating bath proved to be very important, since in its absence it was impossible to prepare solutions of plumbite in NaOH<2.0 M, as PbO was insoluble. Thus, the plating bath containing 0.100 M $Pb^{2+}$, 0.6 M NaOH and 0.2 M glycerol was chosen to perform the following studies of the deposition process, since the solution is less corrosive than 2.0 M NaOH.

To characterize the cathodic process occurring in this bath better, the sweep was reversed at different potentials (Fig. 9).

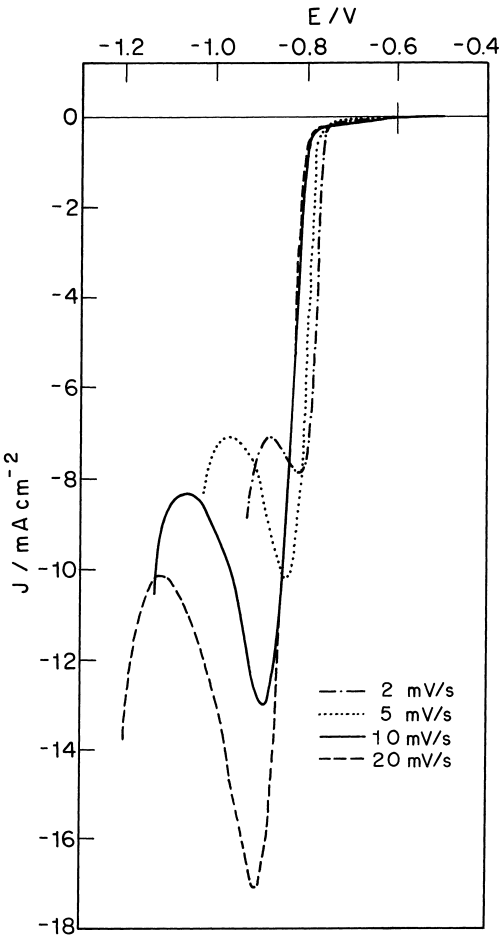


Fig. 10. Voltammetric curves for 1010 steel substrates in 0.100 M $PbNO_3$+2.0 M NaOH+0.2 M glycerol at various sweep rates.

When the sweep was reversed at potential −0.80 V (insert in Fig. 9), an increase in cathodic current and a nucleation loop were observed, suggesting that the metal deposition occurred by nucleation [16]. After the nucleation loop, the cathodic current decreased quickly before the formation

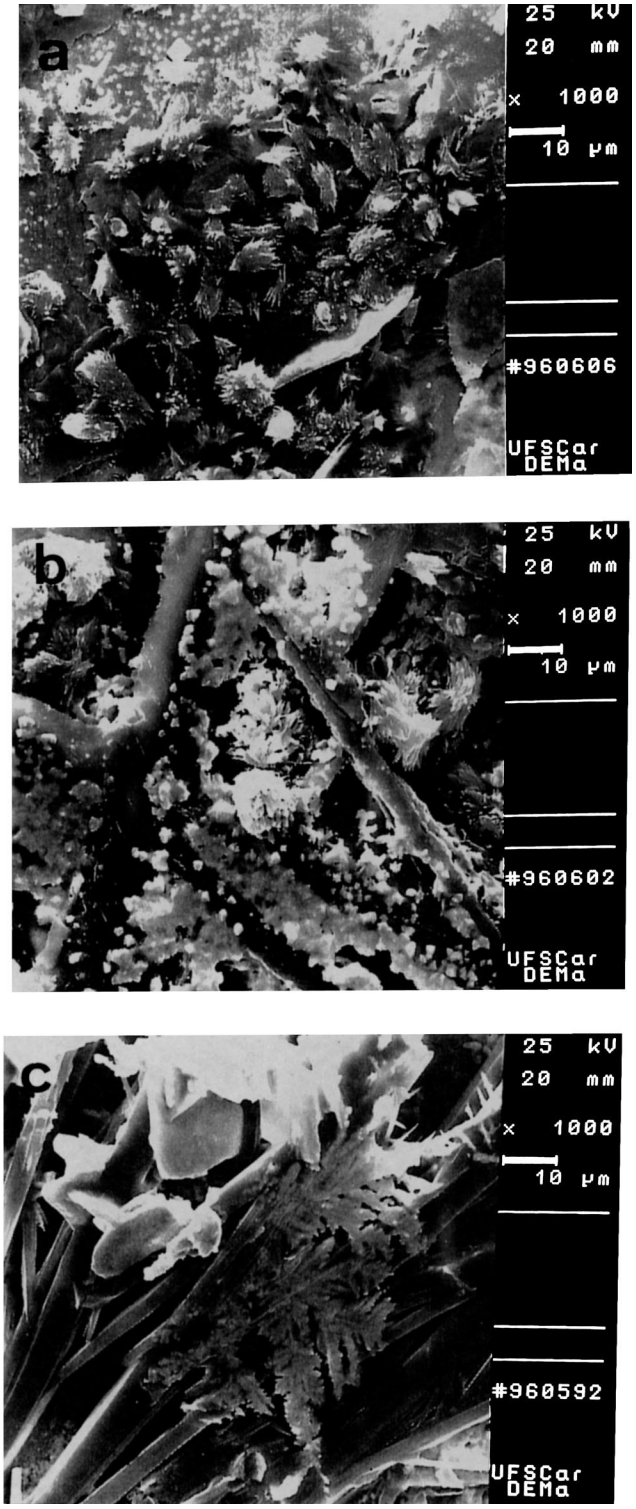


Fig. 11. SEM micrographs for lead films ($v$=10 mV/s) obtained from −0.3 V to various potentials as in Fig. 1: (a) −0.73 V; (b) −0.769 V; (c) −1.05 V. Electrolytic solution: 0.100 M $PbNO_3$+2.0 M NaOH.

of a small anodic peak. When the sweep was reversed at −0.87 V (solid line), the current decreased, indicating that the plating process is under diffusion control [17]. Finally, reversing the sweep at potentials −1.07 V (broken line) and −1.13 V (dotted line), the current increases as in the first case (insert in Fig. 9) indicating a second process of nucleation and growth. Also, it can be verified that in the presence of glycerol there exists a lead nucleation overpotential (∼90 mV), which was not observed in the absence of glycerol.

Fig. 10 shows a set of voltammograms obtained at various sweep rates from a bath containing 0.100 M $Pb^{2+}$, 0.6 M NaOH and 0.2 M glycerol. Results similar to those without glycerol were obtained (Fig. 6).

Lead electrodeposition studies with RDE were made and similar results to those in the absence of glycerol (Fig. 7) were obtained and these confirm that the deposition process is controlled by mass transport.

Finally, it can be concluded from the potentiodynamic curves for the 1010 steel electrode in the Pb plating baths, both in the presence and absence of glycerol, that initial deposition rates are very high. Thus, the growth rate of the crystallites is higher than the nucleation rate and also control by diffusion is established fast; as a consequence, bulky deposits without adherence occur. This is probably due to the high conductance of the electrolyte and the absence of any Ohmic drop.

### 3.3. Study of morphology in the absence of glycerol

Fig. 11a–c show the photomicrographs of lead films obtained by SEM. In the potential range from −0.30 to

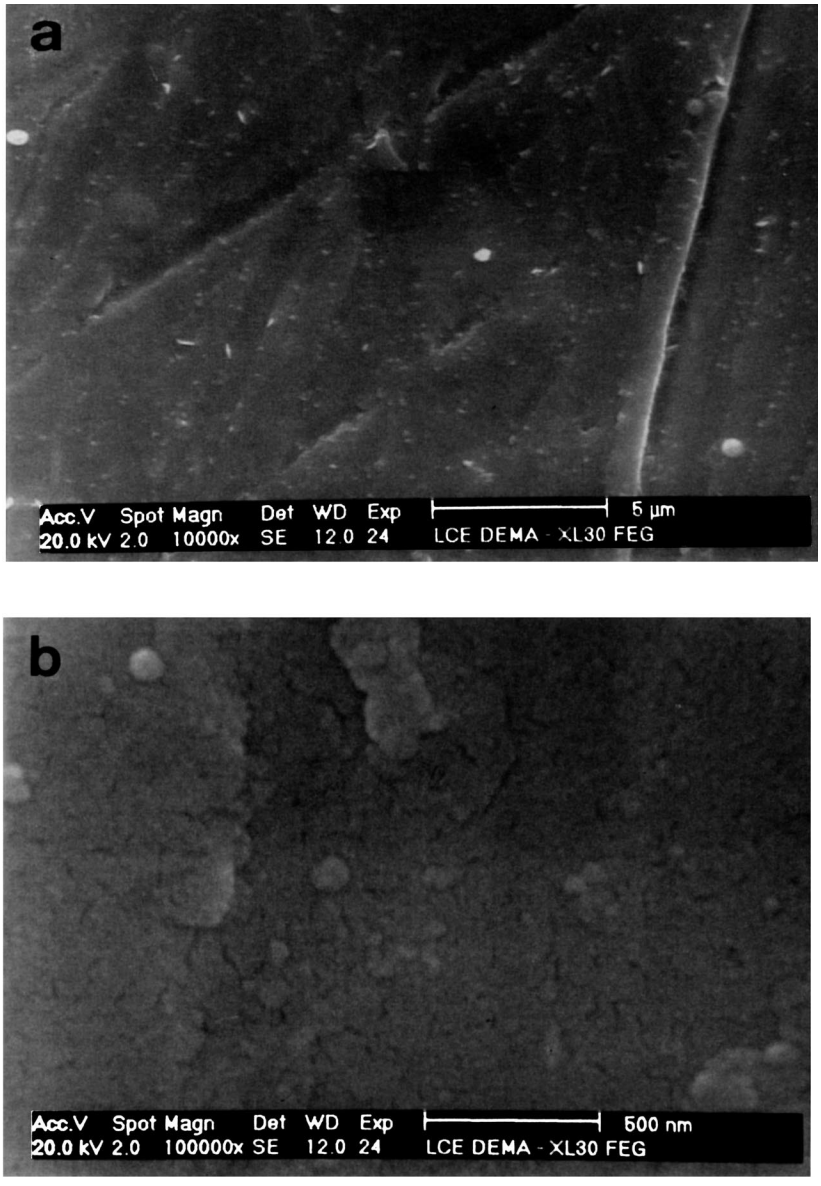


Fig. 12. SEM micrographs for lead films ($v$=10 mV/s) obtained from −0.3 V to $E$=−0.93 V at different magnifications. Electrolytic solution: 0.100 M $PbNO_3$+2.0 M NaOH+0.2 M glycerol.

−0.73 V (Fig. 1d), growth of lead crystallites with a globular, dendrite-like structure, some plates and also small crystallites, were observed (Fig. 11a). This behavior suggests a progressive nucleation mechanism and three-dimensional (3D) growth. During the potential scan from −0.3 to −0.76 V (Fig. 1d), sticks, globular dendrites and coalescence of lead crystallites, could be observed (Fig. 11b). In the potential range from −0.3 to −1.05 V (Fig. 1d), the lead crystallites formed as sticks, ramified dendrites and some plates (Fig. 11c).

### 3.4. Study of morphology in the presence of glycerol

Figs. 12–14 show the physical characterization by SEM of electrodeposited lead films obtained in the presence of glycerol in the plating bath. In the potential range from −0.30 to −0.93 V (Fig. 8, solid line), the substrate was covered in coalesced lead globular crystallites (Fig. 12a and b), which appeared more homogeneous than in the absence of glycerol. During the scan from −0.30 to −1.02 V (Fig. 8, solid line), lead crystallites totally coalesced and dispersed branching dendrites were observed (Fig. 13a), while in the absence of glycerol the aspect of the deposit was more chaotic. Fig. 13b shows the coalescence of lead globular crystallites better. For the potential range from −0.30 to −1.19 V (Fig. 8, solid line), an initial layer of coalesced lead globular crystallites was seen totally covering the substrate, and over these crystallites clusters were scattered (Fig. 14).

These results indicate that the glycerinate anion gives rise to smaller crystallites of lead, at or beyond deposition

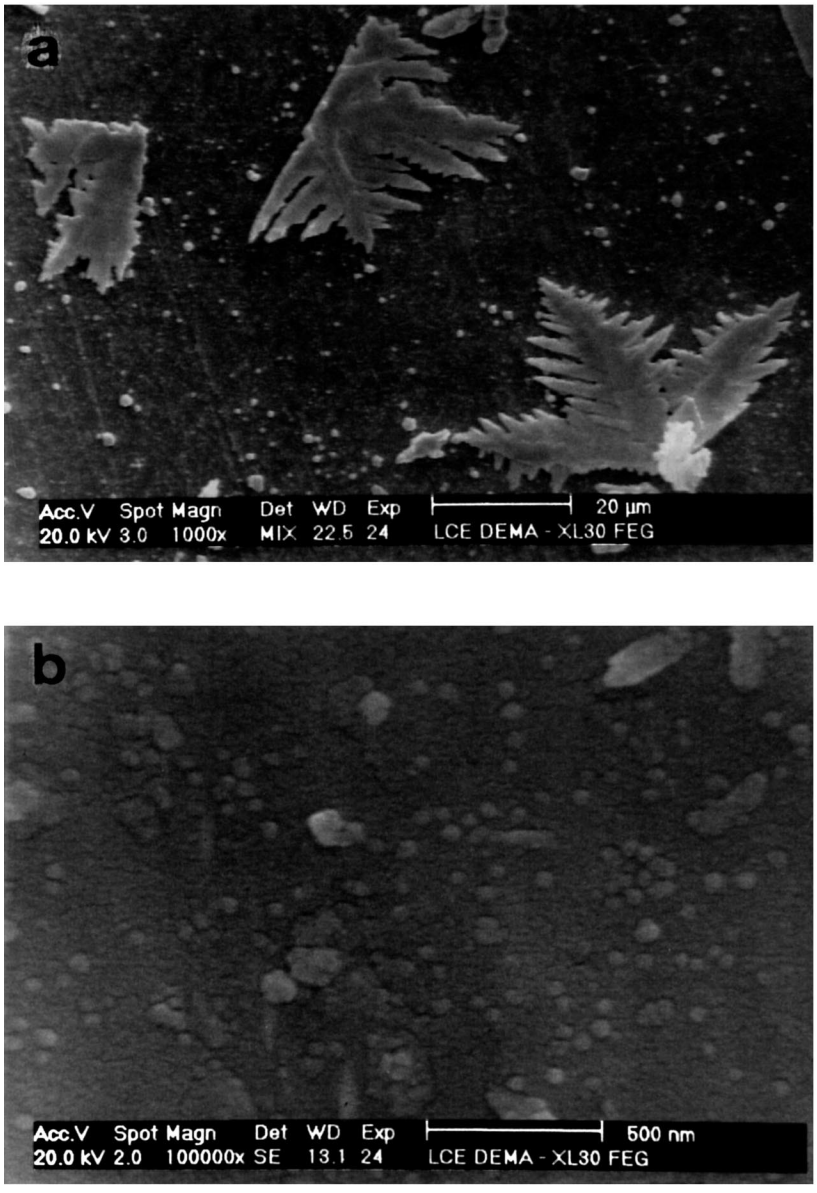


Fig. 13. SEM micrographs of Pb films obtained from −0.3 V to $E$=−1.02 V at different magnifications. Electrolytic solution: 0.100 M $PbNO_3$+2.0 M NaOH+0.2 M glycerol.

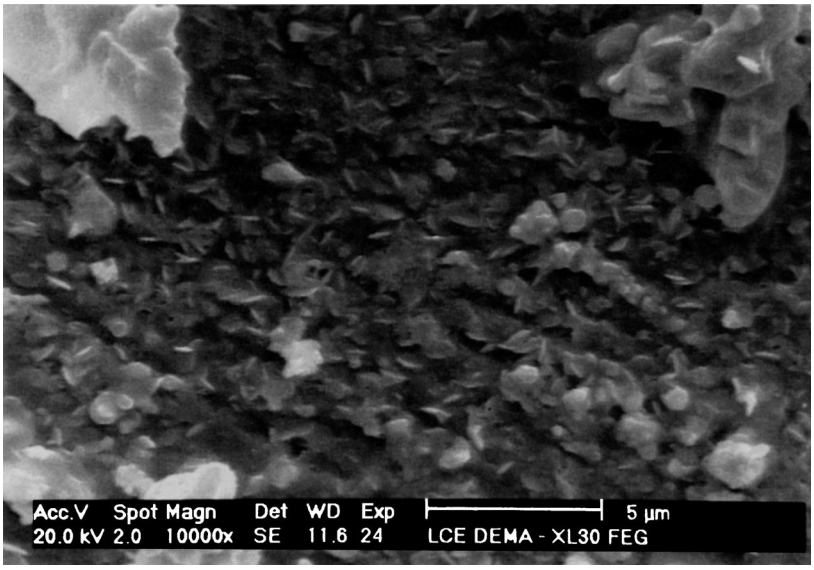


Fig. 14. SEM micrographs of Pb films obtained from −0.3 V to $E$=−1.19 V. Electrolytic solution: 0.100 M $PbNO_3$+2.0 M NaOH+0.2 M glycerol.

potential of around −0.93 V. Thus, it may be inferred that the glycerinate anions act to refine the deposit, principally at a deposition potential of approximately −0.93 V. This point is of great relevance, as it explains the fall in the deposition current density in the region of the cathodic peak (Fig. 8, solid line), where the glycerinate anion works as an effective growth inhibitor, as already noted by other researchers [15]. Also, it may be inferred from these results that, as the presence of glycerol in the plating bath inhibits the propagation of dendrite growth at the deposition potential of approximately −0.93 V, there is probably no need to scrape the lead film to avoid short circuit. Finally, it is unnecessary to use an electrolytic cell of high volume, which has led to a poor total recovery of lead metal.

## 4. Conclusions

Potentiodynamic curves indicated that the lead deposition process is highly catalyzed and controlled by mass transport, leading to production of non-adherent lead film. The undercutting of lead film suggests that an anodic pulse could be used to peel the lead deposits from 1010 steel, allowing a pure lead powder to be collected. The presence of glycerol as an additive in the plating bath modified the current density of the cathodic process, suggesting that this compound affects the morphology of the deposits. From the SEM results, it can be inferred that glycerol has a beneficial effect on the lead deposition, since it reduces the propagation of dendritic growth.

## Acknowledgements

Financial support from Brazilian agencies FAPESP (Proc no. 10145-4/98) CNPq/PIBIC is gratefully acknowledged. Authors want to specially thank Mr. M.A.M.L. Prieto (DEMA–UFSCar) for technical support in SEM experiments.

## References

[1] D. Pavlov, J. Powers Sources 42 (1993) 345.
[2] R. Calusaru, Electrodeposition of Metal Powders, Elsevier, Amsterdam, 1979.
[3] R. Walker, Chem. Ind. 5 (1980) 260.
[4] N.V. Parthasaday, Practical Electroplating Handbook, Prentice-Hall, Englewood Cliffs, NJ, 1989.
[5] D. Pletcher, Industrial Electroplating, Chapman & Hall, New York, 1982.
[6] A.G. Morachevskii, R. J. Appl. Chem. 70 (1) (1970) 1.
[7] F.A. Lowenheim, Modern Electroplating, 2nd Edition, Wiley, New York, 1974.
[8] C. Weiping, T. Yizhuang, B. Kejun, Z. Yue, Trans. Nonferrous Metal Soc. China 6 (4) (1996) 47.
[9] C. Weiping, C. Fancai, P. Yanbing, L. Qizhong, B. Kejun, Z. Yue, Trans. Nonferrous Metal Soc. China 7 (3) (1997) 155.
[10] A.G. Morachevskii, A.I. Demidov, Z.I. Vaisgant, M.S. Kogan, R. J. Appl. Chem. 70 (1) (1970) 1.
[11] I.A. Carlos, R.M. Carlos, C.S. Caruso, J. Power Sources 69 (1997) 37–40.
[12] I.A. Carlos, C.S. Caruso, J. Power Sources 73 (1997) 199–203.
[13] M. Pourbaix, Atlas of Electrochemical Equilibria in Aqueous Solutions, 2nd Edition, National Association of Corrosion Engineers, TX, 1974.
[14] I.A. Carlos, Ph.D. Thesis, Universidade de São Paulo, Brazil, 1990.
[15] M.R.H. de Almeida, Ph.D. Thesis, Universidade Federal de São Carlos, Brazil, 1999.
[16] S. Fletcher, Electrochim. Acta 28 (7) (1983) 917–923.
[17] B.J. Allen, L. Faulkner, Electrochemical Methods: Fundamentals and Applications, Wiley, New York, 1980.